https://doi.org/10.46813/2024-149-103

STRUCTURAL, ELECTRONIC, AND OPTICAL PROPERTIES INVESTIGATION OF ZnSe CUBIC SPHALERITE COMPOUNDS USING DENSITY FUNCTIONAL THEORY (DFT)

Abdulhadi Mirdan Ghaleb[1], Y. Benkrima[2], Asia Qadir Ahmed[1], Zahraa Talib Ghaleb[3]
[1]Department of Physics, College of Science, University of Kirkuk, Kirkuk, Iraq;
[2]Department of Exact Sciences, ENS Ouargla, Algeria;
[3]Department Chemistry, College of Science, University of Kirkuk, Kirkuk, Iraq
E-mail: abdlhadig4@gmail.com

Theoretical investigation of the structural, elastic, electronic and optical properties of ZnSe using the plane-wave pseudo potential formalism method of density functional theory with local density approximation (LDA) and generalized gradient approximation (GGA) as exchange-correlation potentials (DFT). The optimal structure of the binary semiconductor ZnSe crystallized in the complex phase of sphalerite was determined by studying the energy as a function of the basic unit volume. The calculated equilibrium lattice constants, bulk moduli and volumes are in reasonable agreement with the available experimental results. The electronic and chemical bonding properties were investigated by calculating the band structure, density of states and Mulliken population. We found that for ZnSe, the band gap of LDA is 1.33 eV and that of GGA is 1.34 eV. In addition, optical properties (absorption coefficients) were calculated.

PACS: 31.15.E-. 78.20.-e

1. INTRODUCTION

Recently, zinc selenide (ZnSe) has received a lot of attention in potential applications due to its unique physicochemical properties [1–3]: wide band gap, direct transition, low visible light absorption, proper refraction, high conductivity, high photo catalytic activity, environmental friendliness. Due to its large precision binding energy (22 MeV), ZnSe is ideal for manufacturing precision related devices. For example, a ZnSe-based device can be used as follows: green, blue and red light emitting diodes, photo detectors, photo catalysts, solar cells, laser displays, highly optical sensitive devices [4–7]. ZnSe has been investigated experimentally and theoretically intensively using a variety of methods. Theoretical studies include various approximations used to reproduce accurate interpretations of structural and electronic properties obtained from experimental studies. However, different results have led to disagreements between experimenters and theorists. The structural and electronic properties of the material are usually studied theoretically using LDA, GGA, and GW approximations [8, 9]. The results of local density approximation (LDA) and generalized gradient approximation (GGA) [10] underestimate the band gap compared to experimental studies, so GW is the best tool for studying band gap. Is believed to be. However, calculations using the GW approximation are computationally intensive and time consuming. In 2009, Tran and Blaha [11] presented an alternative method for calculating low-cost, time-consuming, and efficient energy band gap. GGA-modified Becke Johnson (mBJ) potential using the Perdew Burke Ernzerhof (GGA-PBE) scheme provides better band gap results. Recently, many empirical and theoretical ab-initio calculations of the structural and electronic properties of ZnX compounds have been performed [12, 13]. Walter et al. [14] calculated the band structure of ZnSe and ZnTe using the empirical pseudopotential method. The rest of the work was divided into three parts. Section 2 briefly describes the computational method used in this study. The most relevant results regarding the structural, elastic, electronic and optical properties of ZnSe compounds are presented and described in Section 3. Finally, Section 4 summarizes the main conclusions of our work.

2. CALCULATION METHOD

The calculations reported in this paper were performed with the plan-wave pseudo potential density functional theory (DFT) method as implemented in the CASTEP code [15], using norm-conserving pseudo potentials [16] and a plane-wave expansion of the wave functions. The exchange-correlation potential was described by LDA with the Ceperley Alder Perdew Zunger (CAPZ) approach can be used to get a rough estimate of E_{xc} [17], and GGA [18] with the PBESOL scheme [19]. Pseudo-atomic calculations are performed on (Zn: $3d^{10}$ $4s^2$), (Se: $4s^2$ $4p^4$). The self-consistent convergence of all energies is $5.0 \cdot 10^7$ eV/atom. Carefully examine the cutoff energy and the dependence of the total energy on the k-point-set mesh after the Monk-Horst-Pack grid to confirm the convergence of the calculation. Considering the computational effort, a plane wave basis set set with an energy cutoff of 460 eV for LDA and 460 eV for GGA is applied and the (6x6x6) (LDA) and (8x8x8) (GGA) k-point Monkhorst Pack mesh is in the Brillouin zone (BZ). Used for BZ, K-point sampling. The convergence criterion of the maximum force between atoms was 0.03 eV/Å, the maximum displacement was 0.001 Å, and the strain was 0.05 GPa. For all equilibrium structures, Mulliken charges were studied using plane wave state projections onto linear combinations of sets of atomic orbitals commonly used to perform charge transfer and

population analysis [20, 21]. Electronic band structure, density of states (DOS) spectrum, and optical characteristics were performed under optimized structure.

3. RESULT AND DISCUSSION

3.1. STRUCTURAL PROPERTIES

Zinc selenide (ZnSe) is a II-VI group compound that crystallizes in sphalerite (space group F43m). The atomic positions of Zn and Se are (0, 0, 0) and (1/4, 1/4, 1/4) in the primitive unit cell, respectively. Fig. 1 shows the crystal symmetry and calculated structural parameters of the investigated compounds. However, Table 1 shows the experimental literature, other theoretical data and the results of our research. The results of the equilibrium lattice constant, bulk modulus, and its pressure derivative are calculated by applying the equilibrium energy and volume result data to the second-order Murnaghan equation of state (EOS) [22]. The results obtained show that our calculations are reasonable.

$$E(V) = E_0 + \frac{B_0 V}{\hat{B_0}}\left[\frac{(\frac{V_0}{V})^{\hat{B}}}{B_0 - 1} + 1\right] - \frac{B_0 V_0}{\hat{B_0} - 1}. \qquad (1)$$

In the above equation, B_0 is the bulk modulus; B_0 is the first derivative with respect to pressure; V_0 is the equilibrium volume at 0 temperature; E_0 is the equilibrium energy of the structure. Examination of the structural properties of ZnSe showed good agreement with the experimental data. This indicates that the use of approximations (LDA and GGA) in structural calculations is appropriate, except for the slightest difference in bulk modules and volume.

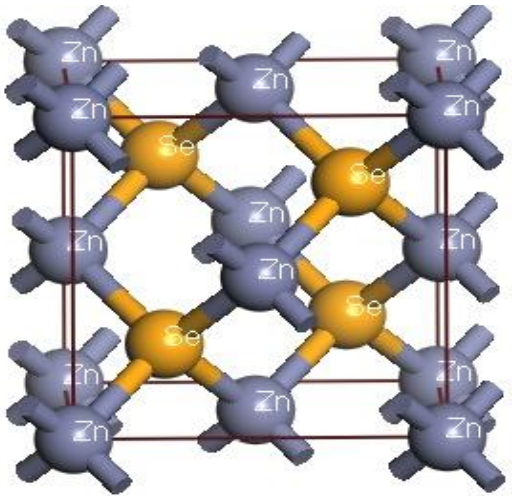

Fig. 1. Crystal structure of Zinc blende ZnSe-compound

Table 1

Values for the lattice constant, bulk modulus, and cell volume of ZnSe compounds

Compound		This work		Experimental work		Other theoretical work	
		LDA	GGA	[23]	[24]	[25]	[26]
ZnSe	α, Å	5.69	5.78	5.66	5.67	5.62	5.63
	B, GPa	77	69.7	69.3	69.3	68.90	72.42
	V, Å	184	193.35	192.4 [27]	–	189.45 [28]	–

3.2. ELASTIC CONSTANTS

The ZnSe three free elastic constants are C_{11}, C_{12} and C_{44} defining the mechanical the material stability. They are often inferred by measuring the total energy which represents the elastic features of the crystal. We can get any stability condition of the cubic crystal through:

$$C_{11} - C_{12} > 0,\ C_{11} + 2C_{12} > 0,\ C_{44} > 0. \qquad (2)$$

$C_{11} > |C_{12}|$ is the first condition, but the first and second states are $C_{11} > 0$. The elastic constant values measured by LDA and GGA (Table 2) meet these stability conditions. Therefore, the ZnSe structure is mechanically stable. Analyzing the results obtained by the two approximations reveals the sequence $C_{11} > C_{12} > C_{44}$. This is consistent with the results of Experiment [29] and Theory [30] in Table 2. However, LDA (GGA) overestimates (underestimates) the experimental values of C_{11} and C_{12} (C_{11}, C_{12}, C_{44}) and underestimates the C_{44} value. The result of the elastic constant shows that the anisotropy coefficient A of ZnSe was obtained by the relational expression (3) [31], which is the calculation of crystal anisotropy. A value of A for a perfectly isotropic material is 1, so a value less than 1 or greater than 1 can be a crystal anisotropy value. The measured A value was 0.39 for LDA and 0.41 for GGA. Therefore, ZnSe is completely isotropic with respect to elasticity, confirming [29] and [30]. These authors state that A has no pressure and is equal to 0.5 in the ZnSe-Zinc blende phase.

$$A = \frac{C_{11} - C_{12}}{2C_{44}}\ . \qquad (3)$$

3.3. ELECTRONIC PROPERTIES

Fig. 2 shows the calculated band structure energies of the binary compounds and their alloys using LDA and GGA. The band structure of ZnSe has a low band energetically separated near -15 eV LDA and GGA, and the minimum value of the conduction band and the maximum value of the valence band are at the G point in the center of the BZ. Yes, we are checking the band gap directly. Interesting points are the shift of the conduction band to higher energies and the wide opening of the band gap. The band gap calculated by LDA and GGA shows the band gap of 1.33 and 1.34 eV, respectively, but the marked band gap is close to the experimental value of 2.96 eV [32]. One of the reasons for the slight difference in energy band gap between theoretical and experimental studies is that current calculations are performed at absolute temperature in the light of DFT and the reported experimental values are at room temperature. These

values were then compared to other theoretical values [33]. The order of band gap energy of ZnSe is that LDA is smaller than GGA, so implementing the LDA potential resolves the band gap and gives results closer to the experimental value [32]. The origin of the energy band structure of a compound is related to the respective densities of the states. Therefore, in order to better understand the energy band gap of ZnSe, total and partial DOS using LDA and GGA was also studied. Near the Fermi level (E_F) in the valence band region is a multiband manifold that is nominally derived from the Se4p state. The valence band is separated from the conduction band by an energy band gap of 1.33 and 1.34 eV at point G of symmetry.

The results are presented in Table 3 and compared with theoretical values and available experimental data. In the case of LDA, it can be seen that the energy difference is underestimated compared with the experimental values. This is because the tendency to approximate local density is known, but the GGA plot provides a very good band gap compared to the test provided by LDA. Results very close to the experimental value (see Table 3) have been significantly improved. Recent calculations show that GGA outperforms other traditional DFT functions for band structure computation. It can be used to model the electronic characteristics of semiconductors.

Table 2

Elastic constant calculated through CASTEP, in GPa units, compared to experimental data and other theoretical calculations

Compound (ZnSe)		C_{11}	C_{12}	C_{44}
Present work	LDA	91.03	59.4	40.56
	GGA	78.4	48.77	36.09
Experimental work [29]		88.8	52.7	41.4
Theoretical work [30]		95.9	53.6	48.9

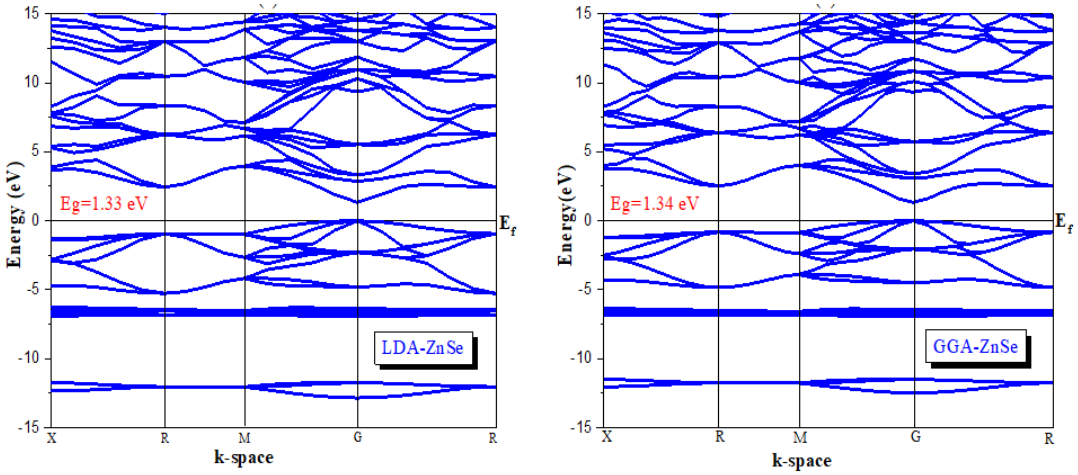

a *b*

Fig. 2. Band gap structure of BZ-ZnSe applying LDA (a), GGA (b)

Table 3

Energy gap value of the ZnSe with the other theoretical and experimental

Methods			
LDA (this work)	GGA (this work)	Other Cal. [33]	Exp. [32]
1.33	1.34	1.07, 1.33	2.96

The origin of the energy band structure of a compound is related to the respective densities of the states. Therefore, to better understand the energy band gaps of ZnSe, the total and partial DOS using LDA and GGA were also investigated. From the band structure (see Fig. 2), the difference in level between the valence band and the conduction band is very small (in terms of energy difference, i.e., the eV band gap is small), which means that ZnSe has a semiconductor. The same tendency is seen from the state density (DOS) (Fig. 3). The band structure in (see Fig. 2) shows the band gap directly. The total expected density of states (PDOS), along with the total DOS, is shown in (Fig. 4). The expected DOS more clearly shows the fundamental contribution of ZnSe to the electronic structure. From Figs. 3 and 4, the structures of DOS are in the -13 and 28 eV energy bands, with the dominant structure having a splitting peak occurring at -6 eV and a small splitting peak between 5 and 10 eV. We would expect the separation in this region to correspond to a spin orbital separation with a value corresponding to the energy value between the two transitions [34]. The inset (see Fig. 3) also shows transitions with sparse energy states with energy ranges of 3 and 28 eV. The projected density of states (PDOS) is calculated based on the dispersion relation and the eigen state pseudo wave function of the KS equation. PDOS is the density of states projected onto the atomic wave function, which more clearly shows its fundamental contribution to electronic structure, as shown in (see Fig. 4). Around

-7 eV pre-peak is observed in Zn3d, Zn4s and Se4p orbitals, with 4p orbitals having higher PDOS values, between -5 and -3 eV, only Se4s and Se4p orbitals have pre-peak. However, in this energy range, Zn3d exhibits a decrease of magnitude 0.00988 eV. At (-5 eV at the Fermi level), a splitting peak is observed in the Zn3d orbital. The peak between the Fermi level and 28 eV (Fermi level shifts to zero) is due to the orbits of Zn4s and Se4p. Therefore, as shown in Fig. 4, both the Zn4s state and the Se4p state contribute significantly to the conduction band due to the hybrid. PDOS to calculate ZnSe uses LDA and GGA. Here, green, red and blue represent the state (d, p, s). In general, the valence band has three main regions. The depth comes from the Se2s state, the center comes from the Zn3d state, part comes from the Se2p state, and the shallow region comes from the Se2p state. The conduction is controlled by the Zn4s and Se2p states. The valence band is mainly controlled by the d state (Zn atom), and the contribution increases in the order of LDA > GGA. Increasing the intensity of the GGA calculation improves the band structure treatment compared with the LDA method presented in (see Fig. 4).

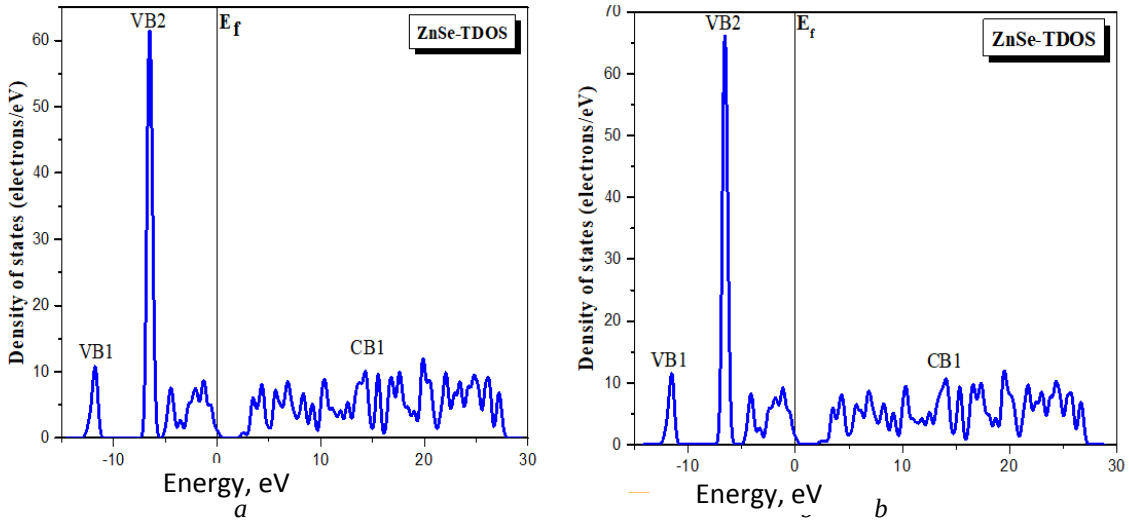

Fig. 3. Total density of states for ZnSe: a – LDA, b – GGA

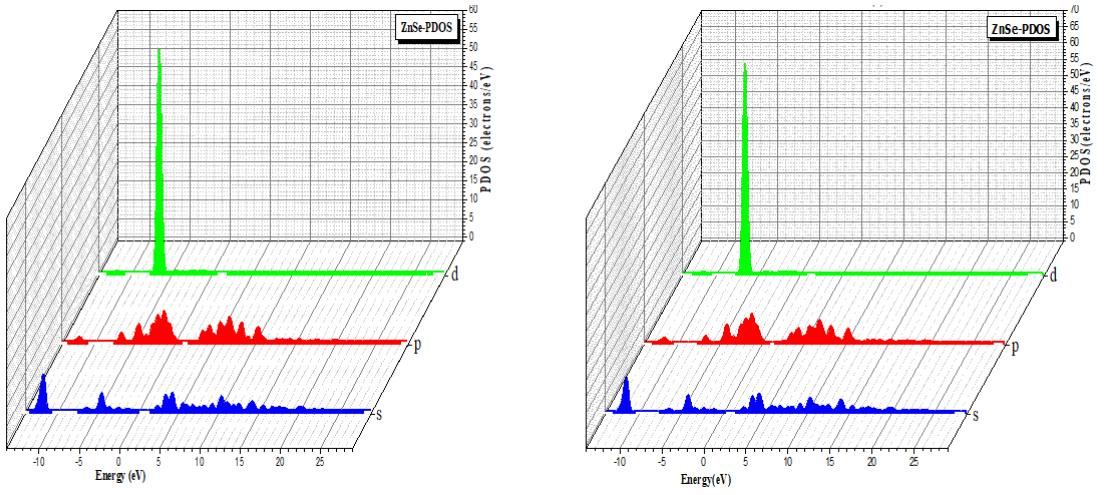

Fig.4. Partial density of state for ZnSe: a – LDA and b – GGA

3.4. OPTICAL PROPERTIES

Optical properties are used to study the interaction between incident photons and ZnSe solid solutions. This supports the setup of photo catalytic reactors with spatial radiation field distribution. Knowledge of the optical properties of solids also helps us to understand their electronic properties. When an object is absorbed a photon, it causes an electrical jump from the occupied state in the valence beam to the empty state in the conduction band (Fig. 5), show the spectrum of the optical absorption coefficient of the compound. have learned. These characterization studies were performed in the chosen energy range of 0…35 eV using both DFT (LDA) and DFT (GGA) while absorption spectroscopy determines the ability of the material to collect or holding incident light or electromagnetic radiation, the absorption values of 2.75E5 cm^{-1} and 2.69E5 cm^{-1} were measured at optical peaks of 7.5 and 9 eV respectively for LDA and GGA. The absorbance calculated by GGA shows a higher absorbance compared to the LDA approximation, which is in good agreement with the experimental absorbance value 16.4E5 cm^{-1} and optical

peak 9.8 eV [35]. The absorption spectrum peaks at low energy levels, while the strong light absorption peaks are primarily in the high energy (5…10 eV) region corresponding to the midband transition. In contrast, there is a positive correlation between reduced absorption and the energy of photons in the high energy range (greater than 10 eV) where electron response is difficult. Therefore, the electrons of VB can be excited to CB by the absorption of visible light. As shown in (see Fig. 5), the strong light absorption spectrum of the zinc blend ZnSe was seen in the UV range (range of incident photon energies from 5 to 40 eV).

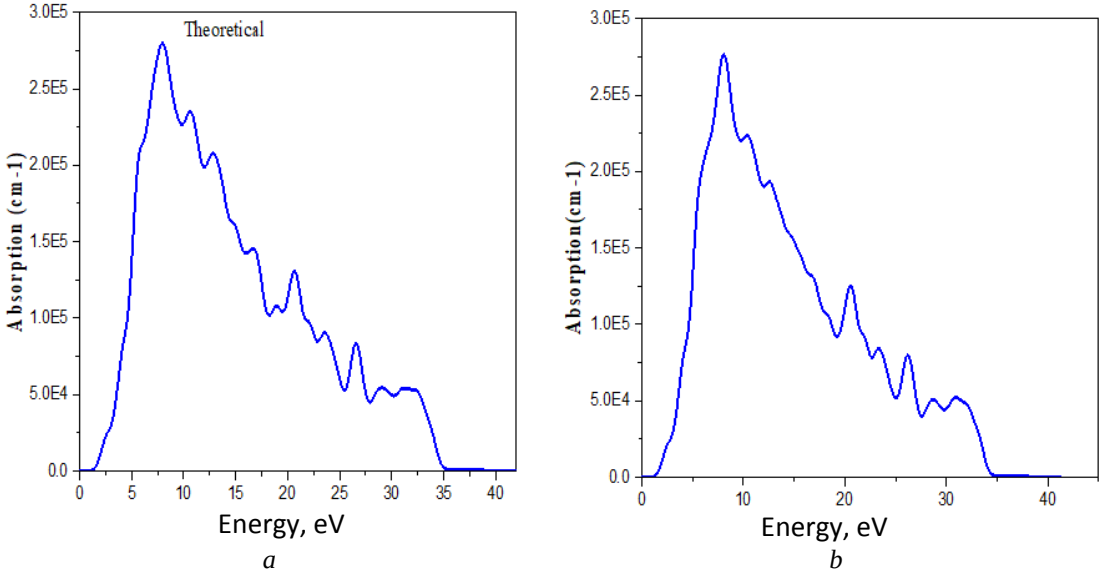

Fig. 5. Absorption coefficient for ZnSe: a – LDA, b – GGA

3.5. CHARGE DENSITY DISTRIBUTION

Using LDA to investigate the nature of the bonding between ZnS atoms, the charge density distribution of valence electrons (e/A^3) in the (3D) and (110) planes is shown in Fig. 6. The color scale in the middle of the map represents the local electron density. Red and blue indicate the lowest and highest electron density, respectively. The charge density distribution map above shows that the charge distribution is centered on the Se atom species and is heavily distorted from the sphere due to the surrounding Zn atom charge distribution. This shows a covalent bond. Since the charge of the Se atom is higher than the charge of the Zn atom, there is also the contribution of ions. Charge density distribution map. There are clear signs of covalent bonding of Zn-Zn, Zn-Se, and Se-Se atoms to ZnSe compounds. These results confirm Mullikan's bond population analyzes (Section "Bond Population Analysis") for 3D and plane (110). The ZnSe charge density map shows that the Zn atom has a higher electron density than the Se atom. Zn and Se atoms are both electron deficient in ZnSe which has a spherical charge distribution. These characteristics imply an ionic contribution to the entire bond, important for understanding the structure and bonding chemistry in crystalline materials. It is also an additional way to understand the electronic structure of a crystal. The calculated charge density distribution is shown in Fig. 6, which shows the intuitive nature of the chemical bonds present in ZnSe. The results show a spherical charge density around the zinc ions, but a small bonding charge inside the selenium ion which is a hybridization effect due to the charge sharing of the zinc and selenium sp orbital's.

3.6. BOND POPULATION ANALYSIS

Two analyzes of the Mulliken population (MPA) [36] were used to further study the binding properties of ZnSe compounds. The results are presented in the Tables 4 and 5. According to MPA, in ZnSe, the Zn atom provides 0.14 and 0.1 charge to each Se atom. As usual, Mulliken charges and overlapping populations are designed to estimate the relative strength of chemical bonds between atoms. We also used effective valencies [21] to determine the predominance of covalent or ionic bonds. This covalent bond is a perfect ionic bond with zero value, while the corresponding bond is larger than this symbolic bond if the bond becomes covalent. Table 4 shows the overall and effective valence charge of the Zn and Se ZnSe grades. The transferred charges of Se and Zn are approximately -0.14 e, 0.14 e in LDA and -0.1 e and 0.10 e in GGA. Therefore, the binding behavior of ZnSe exists together with its covalent and ionic nature. Table 5 shows the measurement results of the Mulliken bond population and bond length of ZnSe using the LDA and GGA functions. The values of the negative and positive binding populations are related to the binding and binding state of the ants. The ZnSe (LDA) Mulliken binding population is 2.46435 Å (2.42839 Å for GGA), which corresponds to a smaller LDA value than GGA. These results confirm the analysis of the electronic structure and density of the above states.

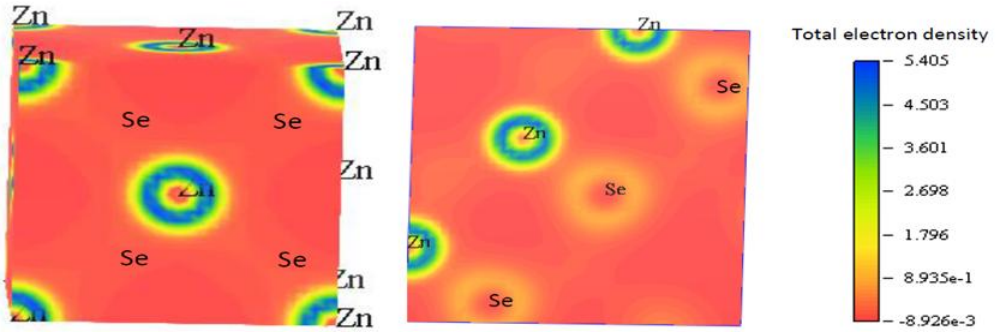

a *b*

Fig. 6. Charge density distribution map of ZnSe: a – (3D) and b – (110) planes using LDA

Table 4

Orbital charges (electron), total charge and atomic Mulliken charge (electron) of ZnSe using LDA and GGA

Methods	Species	s	p	d	f	Total	Mulliken charge (e)
LDA	Se	1.67	4.47	0.00	0.00	6.14	-0.14
	Zn	0.74	1.14	9.98	0.00	11.86	0.14
GGA	Se	1.61	4.50	0.00	0.00	6.10	-0.10
	Zn	0.76	1.16	9.98	0.00	11.90	0.10

Table 5

Calculated bond overlap populations and bond lengths, Å for ZnSe using LDA and GGA

Methods	Bond	Population	Length, Å
LDA	Zn-Se	0.42	2.46435
GGA	Zn-Se	0.29	2.42839

CONCLUSIONS

In summary, ZnSe structural parameters, elastic constants, electronic structures, optical properties, charge density distributions, and bonding population analysis were obtained using density functional theory using local density approximation and general gradient approximation. The most relevant conclusions are summarized as follows: (i) the calculated ground state properties such as lattice parameter, bulk modulus and volume and elastic constants C_{ij} agree quite well with the available experimental and theoretical results. (ii) Our results for the band structure, DOS, and PDOS show that these compounds are semiconductors with a direct band gap (G–G) equal to about 1.33 eV (LDA) and 1.34 eV (GGA) for ZnSe. (iii) Results obtained for energy band gaps using GGA are larger than that within LDA. (iv) The optical properties (absorption coefficient) were investigated in the energy range 0…40 eV. (v) The analysis of the profiles of densities of the electronic states and the density of the electronic charges shows that the structure presents some bonds which are both covalent and ionic. And (vi) Based on the calculations of the density of states and Mulliken population, the chemical bonding indicated both ionic and covalent bonding in ZnSe.

REFERENCES

1. K. Ou, Sh. Wang, L. Bai, et al. Investigation on annealing temperature-dependent optical properties of electron beam evaporated ZnSe thin films // *Thin Solid Films*. 2019, v. 669, p. 247-252.

2. D. Shikha, V. Mehta, J. Sharma, R.P. Chauhan. Electrical characterization of nanocrystalline SnSe and ZnSe thin films: effect of annealing // *Journal of Materials Science: Materials in Electronics*. 2018, v. 29(16), p. 13614-13619.

3. S.A. Hassan, S. Bashir, K. Zehra, Q.S. Ahmed. Structural, morphological and optical properties of pulsed laser deposited ZnSe/$ZnSeO_3$ thin films // *Materials Research Express*. 2018, v. 5(4), p. 046404.

4. S.H. Lee, C. Jung, Y. Jun, S.W. Kim. Synthesis of colloidal InAs/ZnSe quantum dots and their quantum dot sensitized solar cell (QDSSC) application // *Optical Materials*. 2015, v. 49, p. 230-234.

5. Z. Peng, Y. Liu, Y. Zhao, et al. ZnSe passivation layer for the efficiency enhancement of CuInS2 quantum dots sensitized solar cells // *Journal of Alloys and Compounds*. 2014, v. 587, p. 613-617.

6. R. Kondrotas, M. Colina, M. Guc, et al. Towards In-reduced photovoltaic absorbers: Evaluation of zinc-blende CuInSe2-ZnSe solid solution // *Solar Energy Materials and Solar Cells*. 2017, v. 160, p. 26-33.

7. J. Zhu, Y. Koltypin, A. Gedanken. General sono-chemical method for the preparation of nanophasic selenides: synthesis of ZnSe nanoparticles // *Chemistry of Materials*. 2000, v. 12(1), p. 73-78.

8. W.G. Aulbur, M. Städele, A. Görling. Exact-exchange-based quasiparticle calculations // *Physical Review B*. 2000, v. 62(11), p. 7121.

9. M. Shishkin, M. Marsman, G. Kresse. Accurate quasiparticle spectra from self-consistent GW calculations with vertex corrections // *Physical review letters*. 2007, v. 99(24), p. 246403.

10. F. Aryasetiawan, O. Gunnarsson. The GW method // *Reports on Progress in Physics*. 1998, v. 61(3), p. 237.

11. F. Tran, P. Blaha. Accurate band gaps of semiconductors and insulators with a semilocal

exchange-correlation potential // *Physical Review Letters*. 2009, v. 102(22), p. 226401.

12. S.Z. Karazhanov, P. Ravindran, A. Kjekshus, et al. Electronic structure and optical properties of Zn X (X= O, S, Se, Te): A density functional study // *Physical Review B*. 2007, v. 75(15), p. 155104.

13. M.Z. Huang, W.Y. Ching. Calculation of optical excitations in cubic semiconductors. I. Electronic structure and linear response // *Physical Review B*. 1993, v. 47(15), p. 9449.

14. P. Ravindran, P. Vajeeston, A. Ulyashin, et al. Phase stability, electronic structure, and optical properties of indium oxide polytypes // *Phys. Rev. B*. 2007, v. 76, p. 075129.

15. M.D. Segall, P.J. Lindan, M.A. Probert, et al. First-principles simulation: ideas, illustrations and the CASTEP code // *Journal of Physics: Condensed Matter*. 2002, v. 14(11), p. 2717.

16. D. Vanderbilt. Soft self-consistent pseudopodtentials in a generalized eigenvalue formalism // *Physical review B*. 1990, v. 41(11), p.7892.

17. S.H. Vosko, L. Wilk, M. Nusair. Accurate spin-dependent electron liquid correlation energies for local spin density calculations: a critical analysis // *Canadian Journal of Physics*. 1980, v. 58(8), p. 1200-1211.

18. J.P. Perdew, J.A. Chevary, S.H. Vosko, et al. Atoms, molecules, solids, and surfaces: Applications of the generalized gradient approximation for exchange and correlation // *Physical Review B*. 1992, v. 46(11), p. 6671.

19. J.P. Perdew, A. Ruzsinszky, I. Csonka, O.A. Vydrov, G.E. Scuseria, L.A. Constantin, X. Zhou, K. Burke // *Phys. Rev. Lett*. 2008, v. 100, p. 136406.

20. D. Sanchez-Portal, E. Artacho, J.M. Soler. Projection of plane-wave calculations into atomic orbitals // *Solid State Communications*. 1995, v. 95(10), p. 685-690.

21. M.D. Segall, R. Shah, C.J. Pickard, M.C. Payne. Population analysis of plane-wave electronic structure calculations of bulk materials // *Physical Review B*. 1996, v. 54(23), p. 16317.

22. F.D. Murnaghan. The compressibility of media under extreme pressures // *Proceedings of the National Academy of Sciences*. 1944, v. 30(9), p. 244-247.

23. H. Karzel, W. Potzel, M. Köfferlein, et al. Lattice dynamics and hyperfine interactions in ZnO and ZnSe at high external pressures // *Physical Review B*. 1996, v. 53(17), p. 11425.

24. B.H. Lee. Pressure Dependence of the Second-Order Elastic Constants of ZnTe and ZnSe // *Journal of Applied Physics*. 1970, v. 41(7), p. 2988-2990.

25. A. Qteish, M. Parrinello. Stability and structural properties of the SC16 phase of ZnS under high pressure // *Physical Review B*. 2000, v. 61(10), p. 6521.

26. B. Sarkar, A.S. Verma, S. Sharma, S.K. Kundu. First-principles calculations of the structural, phonon and thermal properties of ZnX (X = S, Se, Te) chalcogenides // *Physica Scripta*. 2014, v. 89(7), p. 075704.

27. V. Leute, H. Plate. The Phasediagram of the Semiconductor Alloy ZnkHg (1- k) SelTe (1- l) // *Berichte der Bunsengesellschaft für physikalische Chemie*. 1989, v. 93(7), p. 757-763.

28. S.Z. Karazhanov, P. Ravindran, A. Kjekshus, et al. Electronic structure and optical properties of Zn X (X = O, S, Se, Te): A density functional study // *Physical Review B*. 2007, v. 75(15), p. 155104.

29. B.H. Lee. Elastic constants of ZnTe and ZnSe between 77-300 K // *Journal of Applied Physics*. 1970, v. 41(7), p. 2984-2987.

30. R.A. Casali, N.E. Christensen. Elastic constants and deformation potentials of ZnS and ZnSe under pressure // *Solid state communications*. 1998, v. 108(10), p. 793-798.

31. A. Sadao. *Properties of group-iv, iii-v and ii-vi semiconductors.* Hoboken (USA) Wiley and Sons, 2005.

32. W. Luo, S. Ismail-Beigi, M.L. Cohen, S.G. Louie. Quasiparticle band structure of ZnS and ZnSe // *Physical Review B*. 2002, v. 66(19), p.195215.

33. S.Z. Karazhanov, P. Ravindran, A. Kjekhus, et al. Electronic structure and band parameters for ZnX (X= O, S, Se, Te) // *Journal of Crystal Growth*. 2006, v. 287(1), p.162-168.

34. S.S. Mitra. Phonon assignments in ZnSe and GaSb and some regularities in the phonon frequencies of zincblende-type semiconductors // *Physical Review*. 1963, v. 132(3), p. 986.

35. S. Adachi. *Optical constants of crystalline and amorphous semiconductors: numerical data and graphical information*. Springer Science and Business Media, 2013.

36. R.S. Mulliken. Electronic population analysis on LCAO–MO molecular wave functions // *The Journal of Chemical Physics*. 1955, v. 23(10), p. 1833-1840.

Article received 18.09.2022

ДОСЛІДЖЕННЯ СТРУКТУРНИХ, ЕЛЕКТРОННИХ ТА ОПТИЧНИХ ВЛАСТИВОСТЕЙ СПОЛУК КУБІЧНОГО СФАЛЕРИТУ ZnSe З ВИКОРИСТАННЯМ ТЕОРІЇ ФУНКЦІОНАЛУ ГУСТИНИ (ТФГ)

Абдулхаді Мірдан Галеб, Й. Бенкріма, Асіа Кадід Ахмед, Захра Таліб Галеб

Теоретичне дослідження структурних, пружних, електронних і оптичних властивостей ZnSe з використанням методу формалізму плоскохвильового псевдопотенціалу теорії функціоналу густини з локальною апроксимацією густини (ЛАГ) і узагальненою градієнтною апроксимацією (УГА) як обмінно-кореляційними потенціалами (ОКП). Оптимальну структуру бінарного напівпровідника ZnSe, кристалізованого у складній фазі сфалериту, визначено шляхом дослідження залежності енергії від основної одиниці об’єму. Розраховані рівноважні постійні ґратки, об’ємні модулі та об’єми розумно узгоджуються з наявними експериментальними результатами. Властивості електронного та хімічного зв'язку досліджували шляхом розрахунку зонної структури, щільності станів та населеності Маллікена. Ми виявили, що для ZnSe ширина забороненої зони для ЛАГ становить 1,33 еВ, а для УГА – 1,34 еВ. Крім того, було розраховано оптичні властивості (коефіцієнти поглинання).